

Analysis of P_b centers at the Si(111)/SiO₂ interface following rapid thermal annealing

P. K. Hurley^{a)}

NMRC, Lee Maltings, Prospect Row, Cork, Ireland

A. Stesmans and V. V. Afanas'ev

Department of Physics, University of Leuven, Celestijnenlaan 200 D, 3001 Leuven, Belgium

B. J. O'Sullivan and E. O'Callaghan

NMRC, Lee Maltings, Prospect Row, Cork, Ireland

(Received 11 October 2002; accepted 14 January 2003)

In this work, an experimental study of defects at the Si(111)/SiO₂ interface following rapid thermal annealing (RTA) in a nitrogen ambient at 1040 °C is presented. From a combined analysis using electron spin resonance and quasistatic capacitance–voltage characterization, the dominant defects observed at the Si(111)/SiO₂ interface following an inert ambient RTA process are identified unequivocally as the P_b signal (interfacial Si₃≡Si') for the oxidized Si(111) orientation. Furthermore, the P_b density inferred from electron spin resonance $(7.8 \pm 1) \times 10^{12} \text{ cm}^{-2}$, is in good agreement with the electrically active interface state density $(6.7 \pm 1.7) \times 10^{12} \text{ cm}^{-2}$ determined from analysis of the quasistatic capacitance–voltage response. © 2003 American Institute of Physics. [DOI: 10.1063/1.1559428]

I. INTRODUCTION

It is now well established that interface defects with characteristic peaks in the energy gap are present for polysilicon/SiO₂/Si structures, which are exposed to rapid thermal annealing (RTA) ($T \geq 800$ °C) in an inert ambient as the final process step. The interface density peaks are manifest as peak features in the capacitance–voltage ($C-V$) response of the structure.^{1–7} The peak features in the $C-V$ response are also measured for oxide layers formed by rapid thermal oxidation (RTO), where the $C-V$ measurement is performed directly following the oxidation process using a mercury or aluminum gate layer.^{8,9}

The measured density of states (DOS) across the energy gap following the RTA or RTO processes, extracted from the quasistatic- $C-V$ (QS- $C-V$) response, yields a peak value located at 0.85–0.88 eV above the valence band for the oxidized Si(100) orientation. The location of the peak in the band gap, and the extracted peak densities $(5.5 \times 10^{12}$ to $1.7 \times 10^{13} \text{ cm}^{-2} \text{ eV}^{-1})$,⁷ suggest that the defects are due to unpassivated $P_{b0}/(P_{b1})$ centers for the oxidized Si(100) surface. Moreover, an experiment using Si(111)/SiO₂ structures exposed to RTA (1040 °C, 20 s in N₂) as the final process step, yielded the two well established peaks in the DOS profile for the P_b center of the oxidized Si(111) orientation.⁸ However, the atomic identification of the interface defects as P_b defects by electron spin resonance (ESR) has not been established in previous publications.

The purpose of this article is to examine the interface defects following RTA using ESR, and to compare the ESR density to the electrically active defect density as determined from analysis of the QS- $C-V$ response. The atomic identi-

fication of the interface defects after RTA is important for two main reasons. First, if ESR confirms the interface defects to be P_b centers, then RTA in N₂ is confirmed as an alternative and complementary technique to vacuum annealing ($T \approx 700$ °C, 1×10^{-6} Torr)¹⁰ and rapid furnace pulling¹¹ to dissociate hydrogen from P_b centers to permit electrical or ESR analysis. Second, the identification of the interface defects as P_b centers by ESR, will provide an unambiguous explanation for the peaklike features widely observed in the $C-V$ response of polysilicon/oxide/Si(100) structures measured following RTA in N₂. For this experiment, the Si(111) orientation was selected, as the oxidized Si(111) surface has a well characterized single P_b center^{12,13} as well as clear peaks in the DOS profile in the upper and lower regions of the energy gap.¹⁴

II. EXPERIMENTAL DETAILS

The Si (111) wafers examined in this work were antimony-doped ($1.2 \times 10^{-2} \Omega \text{ cm}$) substrates with a 16[g]mm thick, $6.8 \times 10^{14} \text{ cm}^{-3}$, phosphorous-doped, epitaxial layer. Following a standard clean, the wafers were subjected to dry thermal oxidation at 850 °C in a conventional furnace. The wafers were loaded and stabilized at 850 °C (6.75 slpm N₂ and 0.75 slpm O₂). The oxidation was in pure O₂ (7.5 slpm), with the ramp down to 700 °C and pull in nitrogen (7.5 slpm). The oxide thickness value obtained by ellipsometry was 11.5 nm. Following thermal oxidation, the sample received an RTA at 1040 °C for 20 s in N₂ (subsequently referred to as “RTA only”).

The RTA process had a cooling rate of approximately 35 °C/s. A second sample received the same processing as just detailed, with the addition of a forming gas anneal (FGA) at 450 °C for 30 min in a 15% H₂/85% N₂ ambient

^{a)}Electronic mail: phurley@nmrc.ie

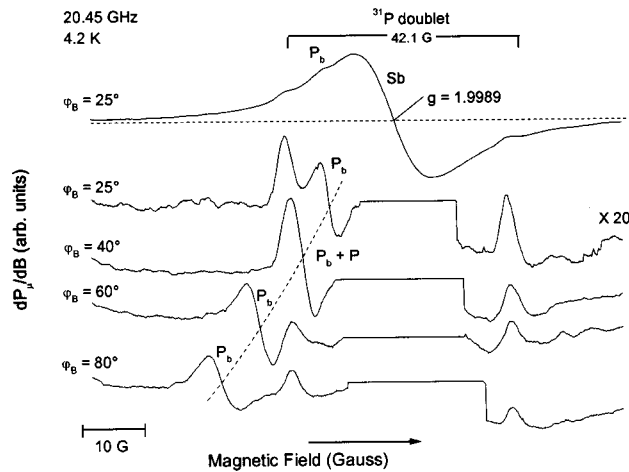


FIG. 1. Absorption-derivative ESR spectra observed on a thermal Si(111)/SiO₂ structure subjected to a postoxidation RTA (1040 °C; 20 s; N₂ ambient) for various angles (φ_B) of \mathbf{B} with the [111] interface normal. Top curve is an as-observed spectrum: For the lower four curves, the intense central signal originating from Sb donors in the Si substrate has been subtracted to better expose the weak P_b and ^{31}P signals. The angular anisotropy of the P_b signal with concomitant broadening is clearly exposed.

following the RTA step. This sample is subsequently referred to as “RTA + FGA.”

The ESR measurements were conventional derivative-absorption K-band (~ 20.45 GHz) $dP_\mu/d\mathbf{B}$ spectra, where P_μ is the incident microwave power and \mathbf{B} the applied magnetic field, recorded at 4.2 K, as described elsewhere.¹² The angle φ_B which \mathbf{B} makes with the sample slice normal \mathbf{n} ($=[111]$) was varied in the range 0° – 90° . Defect densities were determined by comparison of the signal intensity I (area under absorption curve) obtained by double numerical integration of $dP_\mu/d\mathbf{B}$ spectra to that of a comounted LiF:Li ($g=2.002\,293$) reference sample, recorded in one trace. Typically, an ESR sample comprised 20 thinned down slices of $2\times 9\text{ mm}^2$ area each.

QS- C - V characterization was performed using a mercury probe C - V system. The mercury probe area is $4.18\times 10^{-3}\text{ cm}^2$. Precautions were taken to ensure valid quasi-static capacitance data by performing leakage current measurements over the C - V bias range for all samples.

III. RESULTS

Figure 1 shows typical K-band ESR signals observed at 4.2 K on the Si(111)/SiO₂ RTA only sample. Three spectra are observed in a field window of 150 G around the $g\sim 2$ position (marker not included here for clarity). First, there is an intense and broad line centered at $g=1.9989(1)$ of peak-to-peak width $\Delta B_{pp}=15.0\pm 0.2\text{ G}$, dominating the total spectrum. It originates from the occupied (unionized) Sb donors in the highly Sb-doped Si substrate ($\rho=0.012\text{ }\Omega\text{ cm}$). Approximating^{15,16} the magnetic susceptibility χ by a pure Curie law ($\chi\propto 1/T$) for this $S=\frac{1}{2}$ impurity spin system, a density $[\text{Sb}]\sim 1.4\times 10^{18}\text{ cm}^{-3}$ in the substrate is inferred, in fair agreement with the nominal sample resistivity specification ($\rho=0.012\text{ }\Omega\text{ cm}$, $[\text{Sb}]\sim 3.5\times 10^{18}\text{ cm}^{-3}$).¹⁷ When comparing with the P case, the observed large ΔB_{pp} complies with the inferred density.¹⁵

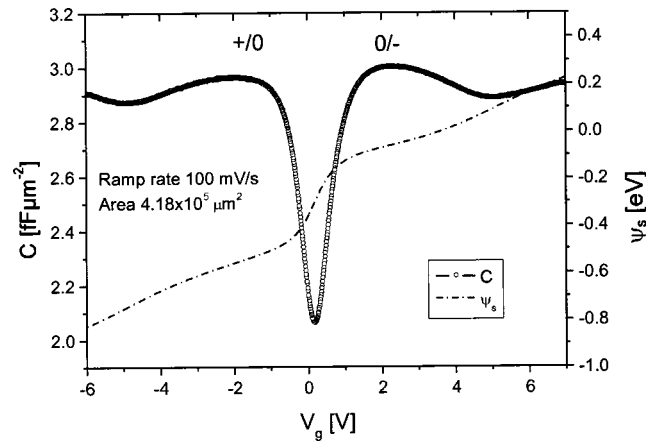


FIG. 2. QS- C - V response (100 mV/s) for the Si(111)/SiO₂(11.5 nm) mercury probe capacitor, with a 1040 °C, 20 s RTA in N₂ as the final process step. The figure also shows the calculated surface potential (ψ_s).

Second, we observe a weak doublet of splitting $a_{hf}=42.1\text{ G}$ centered at $g=1.99840(5)$, originating from^{18,19} the interaction of the localized donor electrons with the ^{31}P ($I=1/2$) nuclei in the P-doped $16\text{ }\mu\text{m}$ thick epitaxial layer on Si doped to $6.8\times 10^{14}\text{ cm}^{-3}$. The doublet signal corresponds to $\sim 3\times 10^{12}$ P spins.

Third, and most interesting, we observe a prominent and unmistakable P_b (interfacial $\text{Si}_3\equiv\text{Si}'$) signal²⁰ of axial symmetry with g matrix principal values $g_{||}=2.0014$; $g_{\perp}=2.0091$. The characteristic anisotropy is clearly exposed in Fig. 1 by varying φ_B from 25° to 80° (four lower curves where the intense Sb signal has been eliminated through simulation to better expose the weak signals), with attendant characteristic increase in ΔB_{pp} with increasing φ_B due to strain-induced line broadening. The inferred P_b density is $(7.8\pm 1)\times 10^{12}\text{ cm}^{-2}$.

The P_b density obtained from the ESR provides a value for comparison to the electrically active defect density obtained from QS- C - V analysis. Figure 2 shows the QS- C - V response of the Si(111)/SiO₂ RTA only sample. The QS- C - V exhibits two peaks (labeled 0/+ and 0/-). The ψ_s versus V_g characteristic is also plotted in Fig. 2, and indicates pinning of the surface potential corresponding to the position of the peaks in the QS- C - V response. The same QS- C - V values are obtained for sweep rates of 25 mV/s, 50 mV/s, and 100 mV/s confirming the effect is not due to non-equilibrium. The two peaks are removed by forming gas annealing (15% H₂, 85% N₂) at 450 °C for 30 min. The DOS across the band gap extracted from the QS- C - V data using the Berglund method is shown in Fig. 3, for the RTA only and RTA + FGA samples. The RTA only sample exhibits two characteristic peaks at 0.31 and 0.84 eV above the valence band edge (E_v). Figure 3 also shows the resulting DOS obtained by subtracting the background U-shaped DOS of the RTA + FGA sample from the RTA only DOS, over the energy range $E_v+0.12\text{ eV}$ to $E_v+1.0\text{ eV}$. From this DOS characteristic, the density associated with the interface defect is determined over the energy range 0.12 to 0.56 eV and 0.56 to 1.0 eV, to be $6.8\times 10^{12}\text{ cm}^{-2}$ and $6.6\times 10^{12}\text{ cm}^{-2}$, respectively. Based on an uncertainty in the oxide thickness of

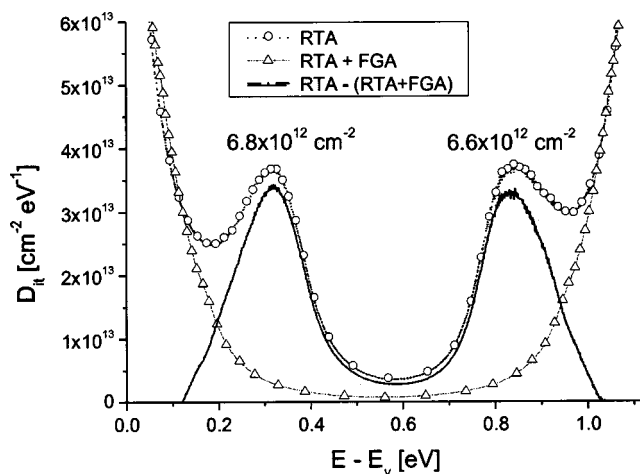


FIG. 3. DOS across the energy gap calculated from the QS-C-V response. Circles: Data calculated for the Si(111)/SiO₂(11.5 nm) mercury probe capacitor, with a 1040 °C, 20 s RTA in N₂ as the final process step (RTA only). Triangles: DOS calculated for the Si(111)/SiO₂(11.5 nm) mercury probe capacitor, with a 1040 °C, 20 s RTA in N₂, and subsequent FGA (450 °C, 30 min, 15% H₂, 85% N₂) (RTA+FGA). Solid line: DOS obtained by subtracting the background U-shaped DOS of the RTA+FGA sample from the RTA only DOS, over the energy range $E_v + 0.12$ eV to $E_v + 1.0$ eV.

± 0.25 nm, this yields an average density of $(6.7 \pm 1.7) \times 10^{12} \text{ cm}^{-2}$ associated with the interface defect following the RTA process.

IV. DISCUSSION AND CONCLUSION

The ESR results confirm that the peak features in the QS-C-V response of metal-oxide semiconductor structures measured directly following RTA in N₂ are the result of unpassivated P_b defects. The density obtained by ESR ($7.8 \pm 1 \times 10^{12} \text{ cm}^{-2}$), is in close agreement with the electrically active density $(6.7 \pm 1.7) \times 10^{12} \text{ cm}^{-2}$ calculated from the QS-C-V response.

A further relevant point is the density of P_b centers obtained from the ESR and QS-C-V analysis. It is well documented,^{12,13} that the interface of as-grown standard thermal Si(111)/SiO₂ is invariably characterized by an inherent P_b density $N_0 = (4.9 \pm 0.4) \times 10^{12} \text{ cm}^{-2}$ for the oxidation range ~ 300 – 950 °C. Interestingly, we find here a markedly higher P_b density, indicating additional creation of P_b centers. Given the final thermal treatment, the sample underwent, i.e., RTA at 1040 °C [effectively a postoxidation anneal (POA) in inert ambient], this result may not come as a surprise. Indeed, as demonstrated previously,¹³ POA in a vacuum or N₂ at elevated temperature may result in strong creation of additional P_b defect sites; e.g., at 1040 °C, P_b densities of $\sim 1.5 \times 10^{13} \text{ cm}^{-2}$ may be attained within minutes.¹³ The value found in the present work is lower, for which there may be several reasons. It may be related to the

very short POA time (20 s) and/or ambient conditions. For one, trace amounts of hydrogenic species in the ambient gas may have resulted in part by the P_b system being left passivated (P_bH formation), i.e., ESR and QS-C-V inactive. Also, there may be an unexplored influence of oxide thickness (only ~ 11.5 nm here). Whatever the case, the important conclusion is that the RTA treatment in N₂ has resulted in depassivation of the P_b centers formed by the oxidation process, and has also generated additional P_b defects. With respect to the Si/SiO₂ interface, this finding confirms the results^{7,8} and unequivocally identifies the origin of the interface traps following inert ambient RTA as unpassivated P_b centers.

ACKNOWLEDGMENTS

The authors would like to acknowledge P. A. Stolk, F. N. Cubaynes, and F. P. Widdershoven of Philips Research Leuven for useful discussions and the provision of the experimental samples.

- ¹A. Kamgar and S. J. Hilenius, Appl. Phys. Lett. **51**, 1251 (1987).
- ²K. Heyers, A. Esser, H. Kurz, and P. Balk, *Proceedings of Insulating Films on Semiconductors 1991*, edited by W. Eccleston and M. Uren (Adam Hilger, New York, 1991), p. 1670.
- ³Y. K. Fang, J. C. Hsieh, C. W. Chen, C. H. Kung, N. S. Tsai, J. Y. Lee, and F. C. Tseng, Appl. Phys. Lett. **61**, 447 (1992).
- ⁴J. C. Hsieh, Y. K. Fang, C. W. Chen, N. S. Tsai, M. S. Lin, and F. C. Tseng, J. Appl. Phys. **73**, 5038 (1993).
- ⁵K. F. Schuegraf, R. P. S. Thakur, and R. Weiner, Proceedings of the International Reliability Physics Symposium (IRPS), Denver, Colorado, April 7–10 (1997), p. 7.
- ⁶P. K. Hurley, C. Leveugle, A. Mathewson, D. Doyle, S. Whiston, J. Prendergast, and P. Lundgren, Mater. Res. Soc. Symp. Proc. **510**, 659 (1998).
- ⁷B. J. O'Sullivan, P. K. Hurley, C. Leveugle, and J. H. Das, J. Appl. Phys. **89**, 3811 (2001).
- ⁸P. K. Hurley, B. J. O'Sullivan, F. N. Cubaynes, P. A. Stolk, F. P. Widdershoven, and J. H. Das, J. Electrochem. Soc. **149**, G194 (2002).
- ⁹J. H. Stathis, D. A. Buchanan, D. L. Quinlan, A. H. Parsons, and D. E. Kotecki, Appl. Phys. Lett. **62**, 2682 (1993).
- ¹⁰M. J. Uren, K. M. Brunson, J. H. Stathis, and E. Cartier, Microelectron. Eng. **36**, 219 (1997).
- ¹¹G. J. Gerardi, E. H. Poindexter, P. J. Caplan, and N. M. Johnson, Appl. Phys. Lett. **49**, 348 (1986).
- ¹²A. Stesmans, Phys. Rev. B **48**, 2418 (1993).
- ¹³A. Stesmans and V. V. Afanas'ev, Phys. Rev. B **54**, R11129 (1996).
- ¹⁴E. H. Poindexter, G. J. Gerardi, M. Rueckel, P. J. Caplan, N. M. Johnson, and D. K. Biegelsen, J. Appl. Phys. **56**, 2844 (1984).
- ¹⁵P. R. Cullis and J. R. Marko, Phys. Rev. B **11**, 4184 (1975).
- ¹⁶Adopting a pure Curie law ($\chi \propto 1/T$) behavior is a first-order approximation of the more realistic Curie-Weiss behavior, i.e., $\chi \propto 1/(T + \theta_a)$, where θ_a is the asymptotic Curie-Weiss temperature. For comparison, the P donor system in Si-doped to $[P] \sim 1.7 \times 10^{18} \text{ cm}^{-3}$ exhibits a Curie-Weiss behavior with $\theta_a = 2.7 \pm 0.3$ K [see A. Stesmans, J. Magn. Reson. **76**, 14 (1988)].
- ¹⁷F. Mousty, P. Ostojia, and L. Passari, J. Appl. Phys. **45**, 4576 (1974).
- ¹⁸G. Feher, Phys. Rev. B **114**, 1219 (1959).
- ¹⁹A. Stesmans and J. Braet, Surf. Sci. **172**, 398 (1986).
- ²⁰K. L. Brower, Phys. Rev. B **33**, 4471 (1986); A. Stesmans and J. Braet, in *Insulating Films on Semiconductors*, edited by J. J. Simone and J. Buxo (North-Holland, Amsterdam, 1986), p. 25.